

## Constraining halo properties from galaxy-galaxy lensing and photo-z

Andreas O. Jaunsen

*European Southern Observatory, Casillo 19001, Santiago 19, Chile*  
*E-mail: ajaunsen@eso.org*

### Abstract

Here we present results from a maximum likelihood analysis of galaxy-galaxy weak lensing effects as measured in a  $12.5 \times 12.5$  field obtained at the Nordic Optical Telescope, on La Palma, Spain. The analysis incorporates photometric redshifts and gives circular velocities consistent with previous weak lensing work.

### 1 Data

The Canada France Redshift Survey (CFRS) 14h-field was observed in May 1998 with the Nordic Optical Telescope (NOT) and the ALFOSC instrument in UBVRI filters. The instrument field is  $7'$  on each side so four pointings were made, covering in total  $12.5 \times 12.5$ . The seeing conditions were good and the measured image qualities in the combined images are  $1''.0$ ,  $1''.0$ ,  $0''.8$ ,  $0''.6$ ,  $0''.6$  in the UBVRI, respectively. The field contains close to 200 galaxies with  $z_{spec}$  from Lilly *et al.*<sup>1</sup> and Koo *et al.*<sup>2</sup>. The  $3\text{-}\sigma$  limiting AB magnitudes are 23.7, 25.1, 25.2, 25.5, 25.1 in the UBVRI, respectively. Objects were only considered when detected in a minimum of three bands, this gave a total of  $\sim 4500$  objects.

### 2 Photometric redshifts

There are two common methods for estimating photometric redshifts. One method relies on a training sample in which the redshifts are known and then a regression is made of the observed colours with the known redshifts. The second method does not need a training sample, but instead uses template spectral energy distributions (SEDs), which are redshifted and fit to the observed colours.

We use the BPZ method as implemented by N. Benitez<sup>3</sup>. This method provides an estimate of the redshift, its uncertainty and the galaxy type. The results are shown in Fig. 1. At around  $z \sim 1$  the scatter increases due to the fact that the main tracer of redshift (the  $4000\text{\AA}$ -break) is redshifted out of the I-band.

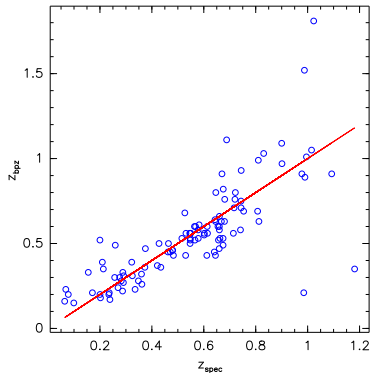


Figure 1: Plot showing the estimated photometric redshift versus the spectroscopic redshift for the sub-sample of galaxies for which this information exists

### 3 Weak lensing measurements

The galaxy shapes are measured using N. Kaiser’s IMCAT software package based on the method described in Kaiser *et al.*<sup>4</sup>. Field distortion was found to be non-negligible due to flexure in the instrument and was corrected by modeling the distortion as a second order polynomial in each image with respect to a reference image taken at the USNO 1.0m telescope (thanks to A. Henden) which is known to have negligible distortion. PSF anisotropies were also identified in the individual images, but varying very smoothly from image to image. Again a second order polynomial model was applied to describe the anisotropy in each image. These models were then combined in to a final model which was used to correct the combined image. The success of this correction is shown in Fig. 2. Finally, seeing effects were normalized by applying the ‘pre-seeing shear polarizability’  $P_\gamma = P^{sh} - \frac{P^{sh(*)}}{P^{sm(*)}} P^{sm}$ , giving the corrected  $e = e' - \gamma P^\gamma$  (Luppino & Kaiser<sup>5</sup>).

### 4 Model

We adopt the simple truncated isothermal sphere model used in Brainerd *et al.*<sup>6</sup>

$$\rho(r) = \frac{V^2 s^2}{4\pi G r^2 (r^2 + s^2)}$$

and the scaling relations used in Hudson *et al.*<sup>7</sup>

$$V = V_* \left[ \frac{L}{L_*(z)} \right]^\eta \quad s = s_{200} \left( \frac{V}{200 \text{ km s}^{-1}} \right)^2 .$$

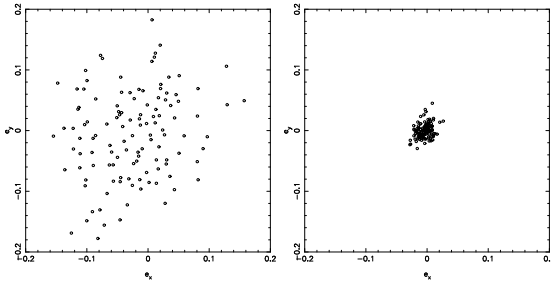


Figure 2: Plots showing the ellipticity vector components for stars before and after correction for the PSF anisotropy

This model is thus used to compute the expected shear for every source galaxy, taking into account all lens galaxies (see definition of lens galaxy in next section). The expected shear is then subtracted from the observed shape of the source galaxy giving the weak lensing corrected ellipticity, which can be compared to the true ellipticity distribution. The latter is assumed to be the best fit gaussian to the observed (raw) ellipticities. We hence maximize the corrected ellipticity distribution with respect to the assumed intrinsic (true) distribution and the likelihood function becomes

$$\log L = \sum_i \left( -\frac{|\epsilon_i - \gamma_i P_j^\gamma|^2}{2\sigma_e^2} \right) ,$$

where  $P_j^\gamma$  is the 'pre-seeing shear polarizability' and  $\sigma_e$  is the best fit Gaussian HWHM. A different shear,  $\gamma_i$ , is obtained by varying the parameters of the model (including scaling relations).

## 5 Results

Lenses are selected as having  $z < z_s + 0.25$ , a maximum  $z < 0.5$  and a projected separation in the lens plane in the range  $25 < r < 150$  kpc. Furthermore, in order to select secure lenses, a final criteria is imposed, namely that the photometric redshift has a probability larger than 95%. Due to the fact that the field is limited and we therefore do not know about the lenses outside the field-of-view for sources close to the edge, we only consider sources more than 150 kpc from the image borders at any given lens redshift. We apply the following cosmological parameters in the analysis:  $\Omega = 0.3$ ,  $\Lambda = 0.7$  and  $h = 1$ . The results are shown as confidence contours in Fig. 3.

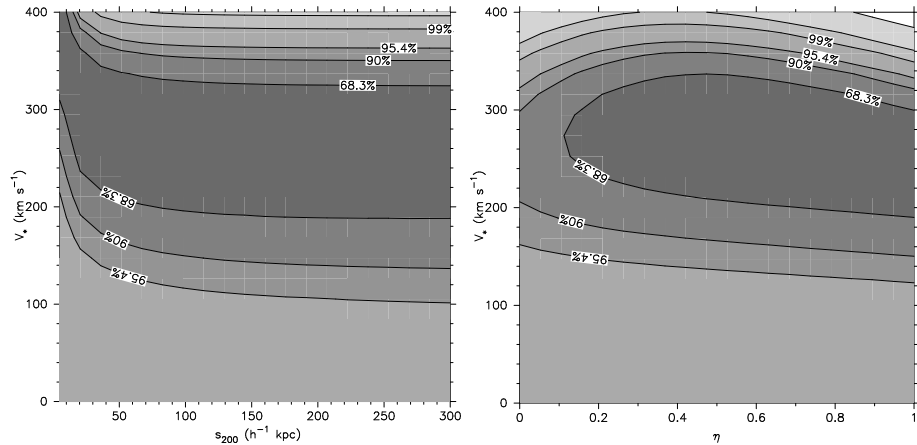


Figure 3: Two-dimensional weak lensing confidence contours on  $V_*$ ,  $s_{200}$  and  $V_*$ ,  $\eta$

The resulting 68.3% conf. level on the circular velocity and the Tully-Fischer exponent is:

$$V_* = 280 \pm 30 \text{ km s}^{-1} \quad \eta = 0.6 \pm 0.4$$

In the near future with photo-z (optical + infrared photometry) and large fields one may explore differences in halo mass, size and scaling relations for different galaxy types and evolution effects.

## References

1. S. J. Lilly, F. Hammer, Le Fèvre O., and Crampton. D. *Astrophys. J.*, 455:50–59, 1995.
2. D.C. Koo, N.P. Vogt, A.C. Phillips, et al. *Astrophys. J.*, 469:535, 1996.
3. N. Benitez. *Astrophys. J.*, 536:571, 2000.
4. N. Kaiser, G. Squires, and T. Broadhurst. *Astrophys. J.*, 449:460, 1995.
5. G. A. Luppino and N. Kaiser. *Astrophys. J.*, 475:20, 1997.
6. T. G. Brainerd, R. D. Blandford, and I. Smail. *Astrophys. J.*, 466:623–637, August 1996.
7. M. J. Hudson, S. D. J. Gwyn, H. Dahle, and N. Kaiser. *Astrophys. J.*, 503:531, 1998.